

## Antibacterial activity of hydrolyzed palm kernel oil and red palm super olein blend against Gram-negative and Gram-positive bacteria

Ilmi Fadhilah Rizki\*, Frisda Rimbun Panjaitan, Manda Edy Mulyono, Brahmani Dewa Bajra

*Mechanization, Post-Harvest and Environmental Conservation Research Group, Indonesian Oil Palm Research Institute, Medan, North Sumatera, Indonesia*

\*Corresponding Author: Ilmi Fadhilah Rizki, Indonesian Oil Palm Research Institute, Medan, North Sumatera 20158, Indonesia. Email: [ilmifadhilahrizki@iopri.org](mailto:ilmifadhilahrizki@iopri.org)

Academic Editor: Charles Okpala, PhD, UGA Cooperative Extension, University of Georgia, Athens, GA 30602, USA

Received: 25 March 2025; Accepted: 2 September 2025; Published: 7 January 2026  
© 2026 Codon Publications

OPEN ACCESS 

ORIGINAL ARTICLE

### Abstract

This study investigated the *in vitro* antibacterial activity of a product, hydrolyzed palm kernel oil (PKO) and red palm super olein (RPSO) blend (HPRB) against Gram-negative (*Escherichia coli* and *Salmonella typhi*) and Gram-positive (*Staphylococcus aureus*) bacteria, all of which are relevant to foodborne illness. HPRB was synthesized through enzymatic hydrolysis of PKO and RPSO at four different ratios. The antibacterial activity of the resulting HPRB formulations was evaluated using disc diffusion and micro-dilution assays. HPRB-C (60% PKO and 40% RPSO) and HPRB-D (80% PKO and 20% RPSO) exhibited the strongest *in vitro* antibacterial activity across all tested bacteria, a finding associated with their high 1-monolaurin content (17.54% and 24.99%, respectively). The phytonutrient content of RPSO also likely contributed to the observed activity. These results suggest that HPRB, particularly formulations C and D, holds promise as a source of natural antibacterial agents, although further optimization for lower effective concentrations and subsequent *in vivo* studies are needed.

**Keywords:** antibacterial activity; red palm super olein; palm kernel oil; monolaurin; phytonutrient

### Introduction

The escalating prevalence of foodborne illnesses and the alarming rise of antibiotic-resistant bacteria have posed a significant threat to global health (M et al., 2020). The spread of antibiotic-resistant genes from foodborne pathogens to more virulent strains increases the potential for severe infections that require extensive medical care. Environmental reservoirs of these resistant strains, especially in settings such as hospitals where antibiotic use is prominent, further broaden their impact (Thamlikitkul et al., 2019). A significant concern is the presence of these resistant bacteria in food production

systems, from where they enter the human food chain (Bale et al., 2024). Bacteria develop resistance to antibiotics through several mechanisms, including the acquisition of resistance genes via horizontal gene transfer (conjugation, transduction, and transformation) and the selection of resistant strains because of antibiotic overuse, which creates an environment where susceptible bacteria are killed and resistant bacteria proliferate. Foodborne pathogens, such as *Salmonella*, *Escherichia coli*, *Listeria monocytogenes*, and *Campylobacter*, have developed resistance to commonly used antimicrobial agents, raising alarms among health experts worldwide (Pranav et al., 2024). Specific resistance mechanisms in

these pathogens include the production of  $\beta$ -lactamases (enzymes that inactivate  $\beta$ -lactam antibiotics), the presence of efflux pumps that expel antibiotics from the cell, ribosomal modifications that prevent antibiotic binding, and target site modification.

Foodborne illnesses, driven by a diversity of microbial pathogens, such as bacteria, viruses, and parasites, have marked implications for public health, healthcare systems, and economic stability. The World Health Organization (WHO, 2016) estimates that millions fall ill each year from foodborne pathogens, with the Southeast Asia region alone experiencing a staggering 150 million cases and over 175,000 deaths annually. The burden of foodborne illnesses is compounded in the Southeast Asia region by several factors, including population density, food handling practices, agricultural systems, and variations in food safety regulations and standards (Wang *et al.*, 2021). For instance, increased urbanization and migration patterns have led to both an increased demand for food and a potential rise in the prevalence of food handling errors, which significantly heighten the risk of transmission of foodborne diseases (Wang *et al.*, 2021). Notably, the WHO emphasizes that foodborne diseases affect individuals in varying degrees of severity, from mild gastrointestinal disturbances to severe health complications resulting in hospitalization or mortality (Lee & Yoon, 2021). The impact of these illnesses is particularly devastating for vulnerable populations, such as young children, the elderly, and the immunocompromised, often leading to severe complications and exacerbating malnutrition (Tao *et al.*, 2022). Vulnerable populations suffering from malnutrition are less equipped to fight off infections, leading to a vicious cycle where foodborne pathogens further impair nutritional status. Malnutrition increases the severity of illnesses, with infected individuals experiencing prolonged recovery period and reduced capacity to absorb essential nutrients (Mulyodarsono & Kristopo, 2024). The situation is further compounded by the limitations of current treatments, including antibiotics, because of the emergence of multidrug-resistant pathogens (Y. Wu & Zeng, 2024).

The urgent need for novel and sustainable antibacterial agents has spurred extensive research into natural products, particularly those derived from plants. Recent trends in this search focus on plant-derived compounds because of their broadspectrum activity, reduced susceptibility to resistance development, potentially fewer adverse effects, and novel chemical structures. Many plant-derived antimicrobials are effective against a wide range of bacteria, including both Gram-positive (e.g., *Staphylococcus* and *Streptococcus*) and Gram-negative (e.g., *E. coli* and *Salmonella*) species. Their reduced susceptibility to development of resistance

is attributed to their multiple mechanisms of action, where these compounds often target different sites in the bacterial cell (e.g., cell membrane, cytoplasm, and genetic material), making it more difficult for bacteria to develop resistance, compared to single-target antibiotics. Plant-derived compounds are often perceived to have lower toxicity compared to synthetic antibiotics. Furthermore, plant antimicrobials often possess unique chemical structures, which can be effective against bacteria that have developed resistance to the existing drugs. Specific examples of plant-derived compounds under investigation include essential oils (e.g., from thyme [thymol], oregano [carvacrol], and tea tree [terpinen-4-ol]), which disrupt cell membranes and inhibit enzyme activity (Martins & Bicas, 2024; Tanasă *et al.*, 2024; Tian *et al.*, 2022); polyphenols (e.g., flavonoids and tannins), which interfere with cell membrane functioning, enzyme activity, and biofilm formation (Takó *et al.*, 2020); and alkaloids (e.g., berberine), which have diverse antibacterial mechanisms, including DNA intercalation and inhibition of cell division (Takó *et al.*, 2020). Pranav *et al.* (2024) and other studies have shown that essential oils and extracts from various plant species exhibit antimicrobial activity against both Gram-positive and Gram-negative bacteria. The ability of plant-derived compounds to target multiple bacterial components simultaneously, such as cell membranes, protein synthesis, and DNA replication, contributes to their efficacy and reduces the likelihood of resistance emergence (Li *et al.*, 2024). Plant-based antimicrobials are often characterized by their favorable safety profiles compared to synthetic antibiotics. Many bioactive compounds derived from plants exhibit lower toxicity and reduced adverse effects, making them more suitable for prolonged therapeutic use (Tsukagoshi *et al.*, 2020). Furthermore, Cheong *et al.* (2022) also emphasized the importance of exploring natural products, including plants, as sources of novel antibacterial agents to address the growing challenge of bacterial resistance.

Palm oil and its derivatives have garnered significant attention among various natural products explored for their antimicrobial potential (Habibiasr *et al.*, 2022; Hovorková *et al.*, 2018). Palm kernel oil (PKO), a widely available and sustainable resource, is rich in medium-chain fatty acids (MCFAs) and is known for its broadspectrum antibacterial activity. PKO contains MCFAs such as lauric acid and myristic acid, which disrupt bacterial cell membranes, leading to cell lysis and death. Lauric acid, a major component of PKO, disrupts bacterial cell membranes by inserting into the lipid bilayer, increasing permeability, and causing leakage of cellular contents. Myristic acid has similar antibacterial properties and may exhibit synergistic effects with other compounds. In their research, Laloučková *et al.* (2019) found that PKO has potential antibacterial

effects against Gram-positive bacteria, including those causing mastitis. Research study conducted by Ustadhi *et al.* (2022) showed that waste palm cooking has an *in vitro* antibacterial effect against *Staphylococcus aureus*. Furthermore, the latest palm oil derivative, red palm super olein (RPSO), contains concentrated phytonutrients, including carotene and vitamin E, which may contribute to their antimicrobial properties (Mulyono *et al.*, 2023). RPSO is rich in phytonutrients, such as carotenoids, vitamin E (tocopherols and tocotrienols), and squalene. Carotenoids may exert antibacterial activity through direct effects on bacteria (e.g., by generating reactive oxygen species [ROS]) or indirect effects through immune modulation. Tocopherols and tocotrienols, forms of vitamin E, possess antioxidant and potential antibacterial properties. Tocotrienols, unlike tocopherols, have unsaturated isoprenoid side chains that may contribute to their biological activity.

Building upon this foundation, the present study focuses on a product, hydrolyzed PKO–RPSO blend (HPRB), created by combining PKO and RPSO through hydrolysis. The unique composition of HPRB, encompassing MCFAs from PKO and phytonutrients from RPSO in a hydrolyzed form, presents a promising avenue for developing a potent and broad-spectrum antibacterial agent with potentially enhanced bioavailability and altered antibacterial properties. This research aims to comprehensively analyze the composition of HPRB and evaluate its antibacterial activity against common human pathogens, including *Staphylococcus aureus*, *Escherichia coli*, and *Salmonella typhi*. Furthermore, the study seeks to identify a specific component within HPRB that is responsible for its antibacterial effects, providing valuable insights for future development and applications.

By elucidating HPRB's antibacterial potential and key components, this study contributes to the growing body of knowledge on natural antimicrobials. The findings may pave the way for developing novel, effective, and sustainable strategies to combat foodborne illnesses and address the pressing challenge of antibiotic resistance.

## Materials and Methods

### Chemicals

The RPSO used in this study was produced in the Oleofood Laboratory at the Indonesian Oil Palm Research Institute (IOPRI, Medan, Indonesia), following the method described by Mulyono *et al.* (2023). This process involves dry fractional crystallization of red palm olein (RPO) to concentrate phytonutrients, such as carotene, vitamin E, and squalene, while also resulting

in a high oleic acid and low palmitic acid content. The PKO was obtained from a local palm oil mill (North Sumatra, Indonesia). The specific details of the palm oil mill, including the variety of palm fruit processed and the extraction methods used, are not available. The chemicals used in this process include the immobilized lipase (Novozymes (N435), Denmark), Mueller Hinton agar (MHA), Mueller Hinton broth (MHB), and 2,3,5-triphenyl tetrazolium chloride (TTC) (Himedia Laboratories Pvt., Mumbai, India). The TTC (1.25%) was prepared with sterile distilled water and stored in sterile flasks covered with aluminum paper at 2–8°C. Tween-80 (Sigma-Aldrich, St. Louis, MO, USA) was used as a solvent.

### Microorganisms

The antibacterial activity of HPRB formulations, alone and in combination with antibiotics (vancomycin and penicillin), was evaluated against the following three bacterial strains: *Escherichia coli* (ATCC 25922), *Staphylococcus aureus* (ATCC 25923), and *Salmonella typhi* (ATCC 1408). These strains were obtained from the Faculty of Medicine, Universitas Sumatera Utara (North Sumatra University), Indonesia. *E. coli* ATCC 25922 is a Gram-negative, non-pathogenic strain commonly used for antimicrobial susceptibility testing. *S. aureus* ATCC 25923 is a Gram-positive strain also frequently used in antibacterial assays. *S. typhi* ATCC 1408 is a Gram-negative bacterium and a causative agent of typhoid fever. Inoculum suspension for each bacterial strain was prepared from 24-h culture colonies grown on MHA. Colonies were suspended in a 0.9% sterile sodium chloride (NaCl) solution, and the bacterial density was adjusted to a turbidity equivalent to 0.5 McFarland standard, corresponding to approximately  $10^8$  colony-forming units (CFU) per milliliter (mL).

### Production of hydrolyzed PKO and RPSO blend

Hydrolyzed PKO and RPSO blend was produced through lipase-catalyzed hydrolysis (Figure 1) using *Candida antarctica* lipase B (Novozymes 435, Denmark) as an enzyme catalyst. Four different HPRB formulations were prepared by mixing PKO and RPSO at the following ratios: HPRB-A (20% PKO and 80% RPSO), HPRB-B (40% PKO and 60% RPSO), HPRB-C (60% PKO and 40% RPSO), and HPRB-D (80% PKO and 20% RPSO). These ratios were chosen to create a systematic variation in the composition of HPRB, allowing us to evaluate the effect of increasing the proportion of PKO (and thus MCFAs such as lauric acid) and decreasing the proportion of RPSO (and its phytonutrients) on antibacterial activity.

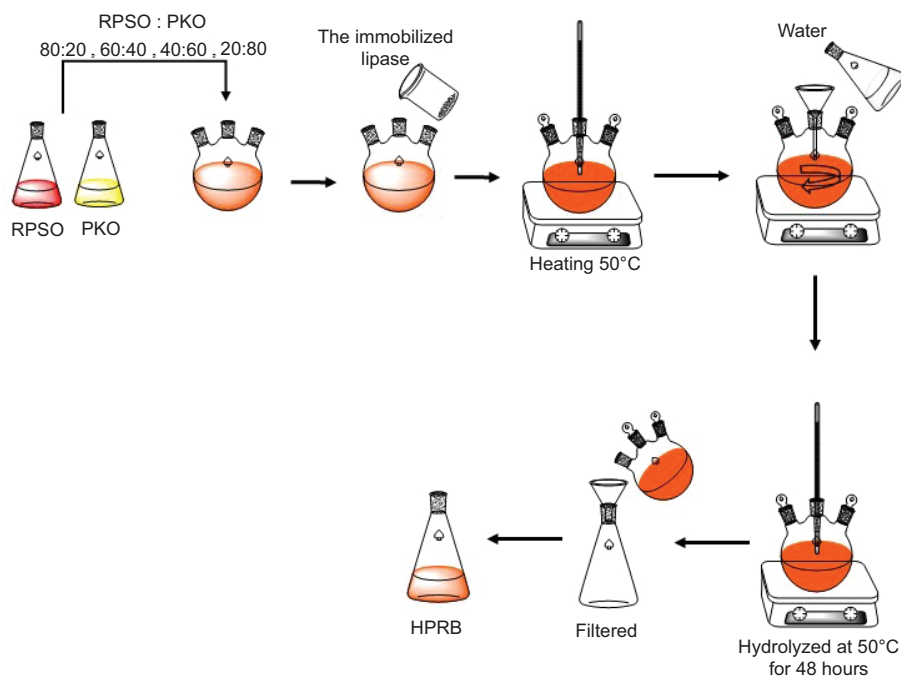


**Figure 1.** A schematic diagram of HPRB production through enzymatic hydrolysis. HPRB: hydrolyzed palm kernel oil and red palm super olein blend; PKO: palm kernel oil; RPSO: red palm super olein.

This systematic variation helps to identify the optimal balance of components. PKO and RPSO were blended according to the desired ratio, and then 8% (w/w) of Novozymes 435 was added. Water was added at 10% (w/w) relative to the total oil weight to initiate hydrolysis. The reaction mixture was stirred continuously using a magnetic stirrer at 200 rpm, and the temperature was maintained at 50°C using a hotplate. Hydrolysis was allowed to proceed for 48 h. Following the reaction, the mixture was filtered to remove immobilized lipase catalyst. The resulting filtrate, containing monolaurin-rich HPRB, was then collected and subjected to further characterization, including analysis of fatty acid, acylglycerol, phytonutrient composition, and lipase residue.

### Characterization of HPRB

#### Composition of fatty acids

The composition of fatty acids was determined as fatty acid methyl esters (FAMES) via gas chromatography (GC)-2010 (Shimadzu, Japan) and a flame ionization detector (FID) equipped with a Shimadzu AOC-20i autosampler (Shimadzu). A DB-23 GC column (Agilent, Santa Clara, CA, USA) was used for separating FAMES. Oven temperature was programmed to increase from 90°C to 208°C at a rate of 7°C/min and then held at 208°C for 5 min. The injector and detector temperatures were set at 260°C. Nitrogen gas was used as the

carrier gas at a flow rate of 1 mL/min. Fatty acid methyl ester standards (Supelco 37-Component FAME Mix) were used for identification and quantification of individual fatty acids. Samples were prepared according to the AOCS Ce 1b-89 method (Collison, 2017). BF<sub>3</sub> was used to convert fatty acids into methyl esters, which are more volatile and readily detectable by GC. The fatty acid composition was expressed as weight percentage (%) of total fatty acids, and analyses were performed in triplicate.

#### Composition of acylglycerol

Composition of acylglycerol was determined using the Shimadzu GCMS-QP2010 Plus (Shimadzu) equipped with a Shimadzu AOC-20i auto-injector (Shimadzu), an Agilent DB-5HT column (Agilent), and helium as a mobile phase at 100 psi. The injector was set at 325°C, while the interface and ion source were set at 280°C. The oven temperature was initially set at 100°C for 1 min, increased to 223°C @ 30°C/min, and later 1°C/min to 227°C. The final increase in temperature was from 5°C/min to 360°C/min for 10 min. Samples were prepared according to AOCS Cd 11b-91 by silyl derivatization with N-methyl-N-(trimethylsilyl)trifluoroacetamide (MSTFA) (Collison, 2017). Acylglycerol standards (Nu-Chek-Prep) were used to identify monoacylglycerols (MAGs), diacylglycerols (DAGs), and triacylglycerols (TAGs). Composition of acylglycerol was expressed as weight percentage (Wt%).

### Squalene

Squalene was analyzed with modification from Wu *et al.* (2022) using Shimadzu GCMS-QP2010 Plus (Shimadzu) equipped with an Agilent HP-5MS column (Agilent). Samples were prepared by saponification in the presence of ascorbic acid to prevent oxidation (Grajzer *et al.*, 2025). The unsaponifiable fraction was injected into gas chromatography–mass spectroscopy (GC-MS) column at a ratio of 1:50 in split injection mode. Helium gas was used at a pressure of 100 psi, while the injector, interface, and ion source temperatures were set at 325°C, 280°C, and 250°C, respectively. The oven temperature was initially set at 50°C for 2 min and increased at a rate of 10°C/min to 300°C/min for 5 min. Squalene standard (Sigma-Aldrich) was used for quantification.

### Total carotene

The HPRB sample was dissolved in hexane and analyzed using a Shimadzu UV-1700 UV–visible spectrophotometer (Shimadzu) at 446 nm according to the Palm Oil Research Institute of Malaysia (PORIM) test method (1995) (Abd Rashid *et al.*, 2019). Total carotene concentration was calculated using the following equation:

$$\text{Total carotene (ppm)} = \frac{383 \times \text{volume} \times \text{absorbance at 446 nm}}{\text{mass of sample} \times 100}$$

The analysis was performed in triplicate using a quartz cuvette with a path length of 1 cm. A standard solution of  $\beta$ -carotene (Sigma-Aldrich) was used for calibration and to confirm the accuracy of measurement.

### Composition of vitamin E

Vitamin E was analyzed with ultra-performance liquid chromatography (UPLC) according to AOCS Ce 8-89 (Waters 600 System, USA), equipped with an autosampler and ultraviolet (UV) detector (Collison, 2017). The analysis was performed using an Inertsil ODS-3 column (Inertsil, USA) with methanol as a mobile phase at a flow rate of 1 mL/min. The injection volume was 20  $\mu$ L, and the UV absorbance was measured at 292 nm. Tocopherol and tocotrienol standards (Sigma-Aldrich) were used for identification and quantification of individual vitamin E isomers (alpha, beta, gamma, and delta).

### Disc diffusion assay of antibacterial activity

The antibacterial activity for all HPRB combinations was determined using the disc diffusion method (Balouiri *et al.*, 2016; “Performance Standards for Antimicrobial Susceptibility Testing 30th Edition,” 2020), and the best formula against *E. coli* (ATCC 25922), *S. aureus* (ATCC

25923), and *S. typhi* (ATCC 1408) were identified (Balouiri *et al.*, 2016). The HPRB combinations were adjusted to different concentrations, such as 10% (250 mg/mL), 30% (500 mg/mL), and 50% (1,000 mg/mL), using Tween 80. The bacterial suspension (0.1 mL) was placed in a 10-mL agar medium test tube, and homogenized to achieve 0.5 McFarland unit turbidity ( $1.5 \times 10^8$  CFU/mL). The suspension was then spread over a petri dish containing solidified MHA using a hockey stick and allowed to dry. Sterilized discs (diameter: 6 mm) were dipped into each HPRB formulation and placed on the agar surface inoculated with respective bacteria. Subsequently, petri dishes were incubated at 37°C for 48 h. Tween 80 was used as a negative control, and two standard antibiotics, penicillin (10 mcg/disc) and vancomycin (30 mcg/disc), acted as positive controls. The antibacterial activity of HPRB was determined based on the diameter of the inhibition zone around the disc.

### Determination of minimum inhibitory concentration (MIC)

The MIC of HPRB formulations was determined using the broth micro-dilution method in 96-well microplates, following the Clinical and Laboratory Standards Institute (CLSI) guidelines with some modifications. *E. coli* (ATCC 25922), *S. aureus* (ATCC 25923), and *S. typhi* (ATCC 1408) were used as test microorganisms. Serial two-fold dilutions of HPRB formulations and control antibiotics were prepared in sterile 96-well microplates. MHB was used as a culture medium. Concentration of HPRB ranged from 2 mg/mL to 1,000 mg/mL, while the antibiotic concentration ranged from 0.5  $\mu$ g/mL to 250  $\mu$ g/mL. MHB, 50  $\mu$ L, was initially added to each well, and then 50  $\mu$ L of the test sample (HPRB or antibiotic) was added to the first well of each row. Serial dilutions were performed by transferring 50  $\mu$ L from the first well to the next well, mixing, and repeating the process down the row. The final 50  $\mu$ L was discarded. Each well was then inoculated with 50  $\mu$ L of bacterial suspension, resulting in a final bacterial concentration of approximately  $5 \times 10^5$  CFU/mL in each well. The microplates were then covered with sterile lids and sealed with parafilm to prevent evaporation. The plates were incubated at 37°C for 24 h under aerobic conditions. Following incubation, 20  $\mu$ L of 0.125% TTC solution was added to each well. The plates were then incubated for an additional 2 h at 37°C. Bacterial growth was indicated by a change to red color, while the absence of red color indicated inhibition of bacterial growth. The MIC was defined as the lowest concentration of HPRB or antibiotic that resulted in no visible color change (i.e., no bacterial growth). Each experiment was performed in triplicate, and the MIC values were recorded for each replicate.

## Bacterial staining assay

After different treatment of MIC procedure, the bacteria suspensions were transferred gently to microscope slide (Smith & Hussey, 2016). The slide was then heated over a gentle flame to help cell adhesion to glass slide and prevent loss of bacteria during rinsing. The Gram staining started with an added crystal violet stain on the slide. After 5 min, the stain was poured off, and the excess stain was rinsed with tap water. Iodine solution was poured over the slide for 1 min and rinsed with tap water. A few drops of decolorizer (mixed solvent of ethanol and acetone) were added to the slide for 10 s and rinsed with tap water. For the last step, the slide was counterstained with fuchsin ( $C_{20}H_{20}N_3 \cdot HCl$ ) solution for 40–60 s and washed off with tap water. The slide was then air-dried and examined under a microscope under oil immersion.

## Statistical analysis

All experiments were conducted in triplicate ( $n = 3$ ), and the results are presented as mean  $\pm$  standard deviation (SD). Statistical differences between groups were analyzed using One-Way Analysis of Variance (ANOVA) with confidence level set at  $P < 0.05$ . Tukey's *post hoc* test

was used to determine significant differences between mean values of groups. All statistical analyses were performed using Statistical Package for Social Sciences (SPSS) version 25 (IN, USA).

## Results

### Characterization of HPRB

#### Fatty acid composition of HPRB

The fatty acid composition of HPRB formulations, along with those of the starting materials PKO and RPSO, was determined using GC with a flame ionization detector (GC-FID). Table 1 shows the fatty acid composition of HPRB, PKO, and RPSO. PKO is characterized by a high proportion of saturated MCFAs, with lauric acid (C12:0) being the predominant fatty acid ( $49.78\% \pm 0.07\%$ ), followed by myristic acid ( $16.02\% \pm 0.01\%$ ). This composition is consistent with the typical fatty acid profile of PKO. In contrast, RPSO is predominantly composed of unsaturated long-chain fatty acids (LCFAs). The most abundant fatty acids in RPSO are oleic acid (C18:1) at  $44.97\% \pm 0.13\%$  and palmitic acid (C16:0) at  $35.91\% \pm 0.15\%$ . This composition reflects the fractionation process that RPSO undergoes, with concentration of oleic acid. The fatty acid profile of HPRB formulations varied depending on the PKO and

**Table 1.** Fatty acid composition (wt%) of HPRB, PKO, and RPSO.

Composition	HPRB-A	HPRB-B	HPRB-C	HPRB-D	PKO (E)	RPSO (F)
C6:0	-	-	0.10 $\pm$ 0.00	0.15 $\pm$ 0.00	0.19 $\pm$ 0.00	-
C8:0	0.60 $\pm$ 0.00	1.17 $\pm$ 0.00	1.82 $\pm$ 0.01	2.42 $\pm$ 0.16	3.16 $\pm$ 0.00	-
C10:0	0.57 $\pm$ 0.00	1.14 $\pm$ 0.01	1.77 $\pm$ 0.02	2.38 $\pm$ 0.13	3.06 $\pm$ 0.00	-
C12:0	8.95 $\pm$ 0.01	18.52 $\pm$ 0.02	28.61 $\pm$ 0.25	39.06 $\pm$ 0.84	49.78 $\pm$ 0.07	0.17 $\pm$ 0.00
C14:0	3.61 $\pm$ 0.00	6.52 $\pm$ 0.00	9.55 $\pm$ 0.02	12.91 $\pm$ 0.06	16.02 $\pm$ 0.01	0.89 $\pm$ 0.02
C16:0	30.98 $\pm$ 0.05	25.78 $\pm$ 0.05	20.32 $\pm$ 0.15	14.27 $\pm$ 0.32	8.21 $\pm$ 0.02	35.91 $\pm$ 0.15
C16:1	0.14 $\pm$ 0.00	0.12 $\pm$ 0.01	0.08 $\pm$ 0.00	-	-	0.17 $\pm$ 0.00
C18:0	3.58 $\pm$ 0.00	3.27 $\pm$ 0.00	2.93 $\pm$ 0.01	2.58 $\pm$ 0.07	2.15 $\pm$ 0.00	3.87 $\pm$ 0.01
C18:1	39.64 $\pm$ 0.06	33.98 $\pm$ 0.00	27.93 $\pm$ 0.10	21.72 $\pm$ 0.57	15.05 $\pm$ 0.02	44.97 $\pm$ 0.13
C18:2	11.23 $\pm$ 0.01	8.91 $\pm$ 0.01	6.41 $\pm$ 0.03	4.11 $\pm$ 0.10	2.16 $\pm$ 0.00	13.23 $\pm$ 0.03
C18:3	0.23 $\pm$ 0.00	0.17 $\pm$ 0.00	0.11 $\pm$ 0.00	0.06 $\pm$ 0.00	-	0.28 $\pm$ 0.00
C20:0	0.28 $\pm$ 0.01	0.24 $\pm$ 0.00	0.19 $\pm$ 0.00	0.15 $\pm$ 0.00	0.08 $\pm$ 0.00	0.33 $\pm$ 0.00
C20:1	0.14 $\pm$ 0.00	0.12 $\pm$ 0.00	0.10 $\pm$ 0.00	0.09 $\pm$ 0.00	0.08 $\pm$ 0.00	0.14 $\pm$ 0.00
$\Sigma$ SFA	48.59 $\pm$ 0.08	56.67 $\pm$ 0.00	65.34 $\pm$ 0.15	73.95 $\pm$ 0.68	82.69 $\pm$ 0.02	41.19 $\pm$ 0.16
$\Sigma$ USFA	51.40 $\pm$ 0.08	43.32 $\pm$ 0.00	34.65 $\pm$ 0.15	25.99 $\pm$ 0.68	17.30 $\pm$ 0.02	58.80 $\pm$ 0.16
$\Sigma$ MUFA	39.93 $\pm$ 0.06	34.22 $\pm$ 0.00	28.12 $\pm$ 0.11	21.82 $\pm$ 0.57	15.14 $\pm$ 0.02	45.29 $\pm$ 0.13
$\Sigma$ PUFA	11.46 $\pm$ 0.01	9.09 $\pm$ 0.01	6.53 $\pm$ 0.04	4.17 $\pm$ 0.10	2.16 $\pm$ 0.00	13.51 $\pm$ 0.03

Notes: HPRB: hydrolized palm kernel oil and red palm super olein blend; PKO: palm kernel oil; RPSO: red palm super olein; C6:0: caproate; C8:0: caprylate; C10:0: caprate; C12:0: laurate; C14:0: myristate; C16:0: palmitate; C18:1: oleate; C18:0: stearate; SFA: saturated fatty acid; USFA: unsaturated fatty acid; MUFA: monounsaturated fatty acid; and PUFA: polyunsaturated fatty acid). Results are reported as mean $\pm$ SD;  $n = 3$ .

RPSO ratios used in their preparation. As the proportion of PKO increased from HPRB-A (20% PKO) to HPRB-D (80% PKO), the levels of lauric acid and myristic acid also increased. Specifically, lauric acid content ranged from  $8.95\% \pm 0.01\%$  in HPRB-A to  $39.06\% \pm 0.84\%$  in HPRB-D, while myristic acid ranged from  $3.61\% \pm 0.00\%$  to  $12.91\% \pm 0.06\%$ . This indicates that the PKO component directly contributes these MCFAs to the HPRB blend.

Conversely, increasing the proportion of RPSO in HPRB formulations led to higher levels of oleic acid and palmitic acid. Oleic acid content ranged from  $21.72\% \pm 0.57\%$  in HPRB-D to  $39.64\% \pm 0.06\%$  in HPRB-A, and palmitic acid content ranged from  $14.27\% \pm 0.32\%$  to  $30.98\% \pm 0.05\%$ . This reflects the contribution of RPSO to the HPRB blend's composition. The total saturated fatty acid ( $\Sigma$ SFA) content was highest in PKO ( $82.69\% \pm 0.02\%$ ) and decreased with increasing RPSO content in HPRB formulations, reaching the lowest level in RPSO ( $41.19\% \pm 0.16\%$ ). Conversely, the total unsaturated fatty acid ( $\Sigma$ USFA) content was lowest in PKO ( $17.30\% \pm 0.02\%$ ) and highest in RPSO ( $58.80\% \pm 0.16\%$ ). The total monounsaturated fatty acid ( $\Sigma$ MUFA) content was highest in RPSO ( $45.29\% \pm 0.13\%$ ), while the total polyunsaturated fatty acid ( $\Sigma$ PUFA) content was highest in RPSO ( $13.51\% \pm 0.03\%$ ). These results demonstrate that the fatty acid composition of HPRB can be tailored by adjusting PKO–RPSO ratio, allowing for the modulation of its MCFA and LCFA content. The high lauric acid content in HPRB formulations with higher PKO content is of particular interest, given lauric acid's known antimicrobial properties.

### Acylglycerol composition of HPRB

The HPRB production process resulted in a unique acylglycerol profile that sets it apart from the original raw materials, PKO and RPSO. This distinction in composition significantly impacts the antibacterial properties of various HPRB formulations. The analysis of acylglycerol composition, as presented in Table 2, highlights diversity in the distribution of different acylglycerol classes across HPRB formulations.

The varying fatty acid profiles of these oils are expected to influence the antimicrobial properties of the resulting HPRB formulations. MCFAs, particularly lauric acid and myristic acid are shown to possess broadspectrum antibacterial activity against various bacteria, including human pathogens bacteria. Therefore, in this study, HPRB was hydrolyzed enzymatically, incorporating both PKO and RPSO, to enrich the composition of fatty acids and their corresponding acylglycerols to enhance the potential antimicrobial activity of these formulations.

HPRB-A stands out with the highest concentration of free fatty acids (14.94%) and TAGs (79.64%). In contrast,

HPRB-D displays a markedly different profile, rich in MAGs (44.93%) and DAGs (24.40%). The abundance of these MAGs might contribute to enhanced antibacterial activity, as certain MAGs are known to disrupt bacterial cell membranes (Jackman *et al.*, 2016). HPRB-C also shows a notable presence of MAGs (30.18%) and DAGs (16.39%), suggesting THAT it could share some of the antibacterial properties of HPRB-D.

The free fatty acid composition of HPRB is primarily characterized by the presence of palmitic acid, oleic acid, and stearic acid. The MAG fraction in HPRB is mainly composed of 1-monolaurin and 1-monomyristin. Notably, HPRB-D boasts the highest levels of both 1-monolaurin (24.69%) and 1-monomyristin (5.91%), while HPRB-C contains the second-highest amount of 1-monolaurin (17.54%). The prevalence of 1-monolaurin is particularly noteworthy due to its potent antibacterial property (Ngatirah *et al.*, 2022). The formation of 1-monolaurin and 1-monomyristin in HPRB is attributed to the partial hydrolysis of PKO and RPSO during the lipase-catalyzed reaction. This process selectively cleaves ester bonds in triglycerides, leading to the generation of MAGs. The specific composition of MAGs is influenced by the fatty acid profile of the starting materials and the selectivity of lipase enzyme (Subroto, 2020).

### Phytonutrient composition of HPRB

The raw materials used to synthesize HPRB have limited nutrients. PKO lacks phytonutrients, while RPSO has low MCFA. Thus, combining PKO and RPSO potentially increases the composition of MCFA and phytonutrients in HPRB. The resulting HPRB in this study exhibited changes in MCFA and phytonutrient contents, and MAG was present as a fatty acid. Table 3 details the phytonutrient composition of each HPRB formulation, PKO, and RPSO, consisting of total carotene, vitamin E and its isomers, and squalene. The RPSO has the highest phytonutrient among oils: total carotene = 761.23 ppm, total vitamin E = 1,118.17 ppm, and squalene = 257.5 ppm. Moreover, RPSO has low palmitic acid (saturated fatty acid) and high oleic acid (unsaturated fatty acid), as shown in Table 2. The presence of double bond is attributed to the high solubility of unsaturated fats. RPSO is the primary source of phytonutrients in HPRB synthesis; thus, composition of phytonutrients increases with inclusion of higher RPSO in the formulation.

### Antibacterial activity of HPRB

#### Disc diffusion assay

The antibacterial activity of HPRB formulations was evaluated by measuring inhibition zone diameters (Table 4). Notably, HPRB-C and HPRB-D demonstrated significantly higher antibacterial

**Table 2.** Acylglycerol composition (wt%) of HPRB, PKO, and RPSO.

Acylglycerol species <sup>b</sup>		HPRB-A	HPRB-B	HPRB-C	HPRB-D	PKO (E)	RPSO (F)
FFA	P	4.42±0.01	7.04±0.19	6.75±0.27	6.11±0.30	ND	ND
	O	9.82±0.44	0.59±0.13	1.52±0.14	3.11±0.06	ND	0.53±0.12
	S	0.70±0.02	1.44±0.14	1.36±0.09	ND	ND	ND
	<b>Total</b>	<b>14.94±0.47</b>	<b>9.07±0.20</b>	<b>9.63±0.20</b>	<b>9.21±0.36</b>	<b>0</b>	<b>0.53±0.12</b>
MAG	-Ca-	ND	ND	ND	0.53±0.06	ND	ND
	Ca--	ND	ND	ND	2.20±0.59	ND	ND
	-La-	ND	0.79±0.06	1.76±0.39	2.30±0.10	ND	ND
	La--	ND	16.95±1.15	17.54±0.72	24.69±1.10	ND	ND
	-M-	ND	ND	ND	0.52±0.03	ND	ND
	M--	1.15±0.09	2.22±0.02	3.61±0.14	5.91±0.12	ND	ND
	P--	0.80±0.08	1.36±0.05	1.10±0.07	2.67±0.24	ND	ND
	O--	1.63±0.14	3.17±0.06	4.70±0.23	5.43±1.18	ND	0.40±0.02
	S--	ND	0.29±0.02	0.58±0.03	0.68±0.16	ND	ND
	<b>Total</b>	<b>3.58±0.15</b>	<b>24.79±1.36</b>	<b>30.18±1.57</b>	<b>44.93±3.09</b>	<b>0</b>	<b>0.40±0.02</b>
DAG	La-Cp	ND	ND	ND	1.27±1.27	ND	ND
	La-Ca	ND	0.61±0.05	0.99±0.05	1.75±0.13	ND	ND
	LaLa-	0.62±0.04	1.52±0.01	2.75±0.13	3.93±0.01	0.15±0.00	ND
	La-La	1.22±0.01	3.52±0.17	6.81±0.01	8.90±0.41	0.44±0.03	ND
	LaM-	ND	0.49±0.02	1.05±0.01	1.78±0.20	ND	ND
	La-M	ND	1.24±0.03	2.33±0.16	3.20±0.61	0.14±0.02	ND
	La-P	ND	0.67±0.01	1.77±0.01	2.46±0.32	0.05 ± 0.05	ND
	LaO-	ND	0.33±0.02	0.71±0.07	1.12±0.10	ND	ND
	P-P	ND	ND	ND	ND	ND	0.12±0.12
	P-O	ND	ND	ND	ND	ND	1.18±0.11
	O-O	ND	ND	ND	ND	ND	0.85±0.19
	<b>Total</b>	<b>1.83±0.06</b>	<b>8.37±0.20</b>	<b>16.39±0.43</b>	<b>24.40±1.94</b>	<b>0.78 ±0.00</b>	<b>2.14 ±0.18</b>
TAG	LaLaCo	ND	ND	ND	ND	0.71±0.06	ND
	LaLaCp	ND	1.11±0.01	2.18±0.00	2.78±0.02	6.61±0.34	ND
	LaLaCa	ND	ND	ND	ND	8.90±0.11	ND
	LaLaLa	2.28±0.03	2.53±0.15	2.10±0.30	2.57±0.75	27.72±0.35	ND
	LaLaM	1.02±0.00	1.34±0.04	1.78±0.35	1.83±0.01	20.58±0.15	ND
	LaLaP	ND	0.17±0.17	0.65±0.01	1.07±0.18	10.37±0.02	ND
	LaLaO	ND	0.31±0.05	0.64±0.02	0.47±0.47	2.71±0.04	ND
	LaMP	ND	ND	ND	ND	5.71±0.04	ND
	LaMO	ND	ND	ND	0.30±0.30	2.97±0.04	ND
	LaMS	ND	ND	ND	ND	2.04±0.00	ND
	LaOP	ND	ND	ND	ND	3.52±0.14	ND
	PPP	0.50±0.04	0.52±0.06	0.57±0.20	0.26±0.2	4.07±0.25	0.10±0.25
	POP	20.19±1.11	12.83±0.33	9.53±0.06	3.68±0.40	1.27±0.04	24.96±1.54
	POO	45.11±1.21	32.02±0.56	20.57±1.77	7.90±1.02	1.07±0.05	56.51±1.85
	OOO	10.55±0.49	6.95±0.73	4.89±0.09	0.59±0.59	0.97±0.09	14.47±0.03
	<b>Total</b>	<b>79.64±0.67</b>	<b>57.77±1.37</b>	<b>43.80±2.21</b>	<b>21.46±0.78</b>	<b>99.23±0.00</b>	<b>96.93±0.04</b>

Notes: HPRB: hydrolized palm kernel oil and red palm super olein blend; PKO: palm kernel oil; RPSO: red palm super olein; FFA: free fatty acid, MAG: monoacylglycerol; DAG: diacylglycerol; TAG: triacylglycerol; Co: caproate; Cp: caprylate; Ca: caprate; La: laurate; M: myristate; P: palmitate; O: oleate; S: stearate; ND: not detected.

The position of fatty acid on glycerol backbone is indicated by the symbol "-."

For TAGs, the notation represents three fatty acids at sn-1, sn-2, and sn-3 positions.

<sup>a</sup>Mean±standard deviation (n = 3).

<sup>b</sup>Some acylglycerols might be undetected due to limit of detection.

**Table 3.** Phytonutrient composition (mg/kg) of HPRB, PKO, and RPSO.

Composition	HPRB-A	HPRB-B	HPRB-C	HPRB-D	PKO (E)	RPSO (F)
Total carotene	604.08±0.74	452.69±1.42	303.29±1.24	165.05±2.33	2.18±1.07	761.23±1.64
Total vitamin E	867.54±3.10	608.19±10.29	251.32±2.51	78.61±1.63	15.60±1.65	1118.17±7.24
$\delta$ -Tocotrienol	142.64±0.88	131.74±1.70	102.46±2.38	49.36±0.43	15.60±1.65	167.11±2.60
$\gamma$ -Tocotrienol	438.12±0.86	336.39±4.95	148.85±2.85	29.24±2.06	-	549.16±2.43
$\alpha$ -Tocotrienol	230.57±1.70	115.16±6.78	-	-	-	313.02±1.43
$\alpha$ -Tocopherol	56.21±0.62	24.88±0.40	-	-	-	88.87±2.74
Squalene	178.5±3.53	131±2.82	87.5±2.12	51±1.41	23.5±2.12	257.5±17.67

Notes: HPRB: hydrolyzed palm kernel oil and red palm super olein blend; PKO: palm kernel oil; RPSO: red palm super olein. Results are reported as mean  $\pm$ SD, n = 3.

**Table 4.** Inhibition zone diameter and minimum inhibitory concentration of HPRB.

Sample	<i>Staphylococcus aureus</i>		<i>Escherichia coli</i>		<i>Salmonella typhi</i>	
	Inhibition diameter (mm)	MIC (mg/mL)	Inhibition diameter (mm)	MIC (mg/mL)	Inhibition diameter (mm)	MIC (mg/mL)
HPRB-A	14.15±0.01 <sup>c</sup>	1,000	13.57±0.14 <sup>a,b</sup>	1,000	10.77±0.05 <sup>a,b</sup>	1,000
HPRB-B	16.4±0.015 <sup>b</sup>	1,000	9.12±0.03 <sup>a,b</sup>	500	13.7±0.00 <sup>a,b</sup>	1,000
HPRB-C	20.4±0.065 <sup>a</sup>	500	10.85±0.03 <sup>a,b</sup>	1,000	14.52±0.21 <sup>a</sup>	500
HPRB-D	19.47±0.05 <sup>a</sup>	250	14.72±0.47 <sup>a</sup>	500	13.87±0.01 <sup>a</sup>	500
PKO (E)	8.65±0.05 <sup>d</sup>	NI*	8.22±0.11 <sup>b</sup>	NI*	12.1±0.26 <sup>a,b</sup>	NI*
RPSO (F)	8±0.1 <sup>d</sup>	1,000	8.55±0.02 <sup>b</sup>	1,000	9.85±0.00 <sup>b</sup>	100
Penicillin	16.7±0.09	15	24.4±0.018	15	23.3±0.067	15
Vancomycin	1.6±0.09	15	12.4±0.04	15	26.75±0.027	15

Notes: HPRB: hydrolyzed palm kernel oil and red palm super olein blend; PKO: palm kernel oil; RPSO: red palm super olein; MIC: minimum inhibitory concentration.

The inhibition zone includes diameter of the disk (6 mm). Values of inhibition diameter are given as mean $\pm$ SD, n = 3.

Different superscript alphabets are significantly different in each column by Tukey's test ( $P < 0.05$ ).

\*NI: no inhibition.

activity compared to other formulations, which exhibited the largest inhibition zones against all three bacterial strains. Specifically, HPRB-C (500 mg/mL) displayed inhibition zones of 20.4 mm, 10.85 mm, and 14.52 mm against *S. aureus*, *E. coli*, and *S. typhi*, respectively. Similarly, HPRB-D (250 mg/mL) showed the respective inhibition zones of 19.47 mm, 14.72 mm, and 13.87 mm against the same strains. The MIC for HPRB-C and HPRB-D was also lower than those for HPRB-A (1,000 mg/mL; 14.15 mm, 13.57 mm, and 10.77 mm) and HPRB-B (1,000 mg/mL; 16.4 mm, 9.12 mm, and 13.7 mm), further supporting their superior antibacterial activity. Both raw materials (PKO and RPSO) showed either no inhibition (NI) or significantly smaller inhibition zones (PKO: 8.65 mm, 8.22 mm, and 12.1 mm; and RPSO: 8 mm, 8.55 mm, and

9.85 mm), compared to HPRB formulations, highlighting the enhanced antibacterial properties achieved through the formulation process.

#### Minimum inhibitory concentration

Figure 2 illustrates the MIC of HPRB against three bacterial strains: *Staphylococcus aureus*, *Escherichia coli*, and *Salmonella typhi*, using a 96-well plate setup with decreasing HPRB concentration and the colorimetric indicator TTC. The red color, indicative of bacterial growth, diminishes with increasing HPRB concentration, allowing visual identification of MIC as the lowest concentration without red color. The figure enables comparison of MICs across strains, revealing varying susceptibilities and the potential of HPRB as an antibacterial agent.

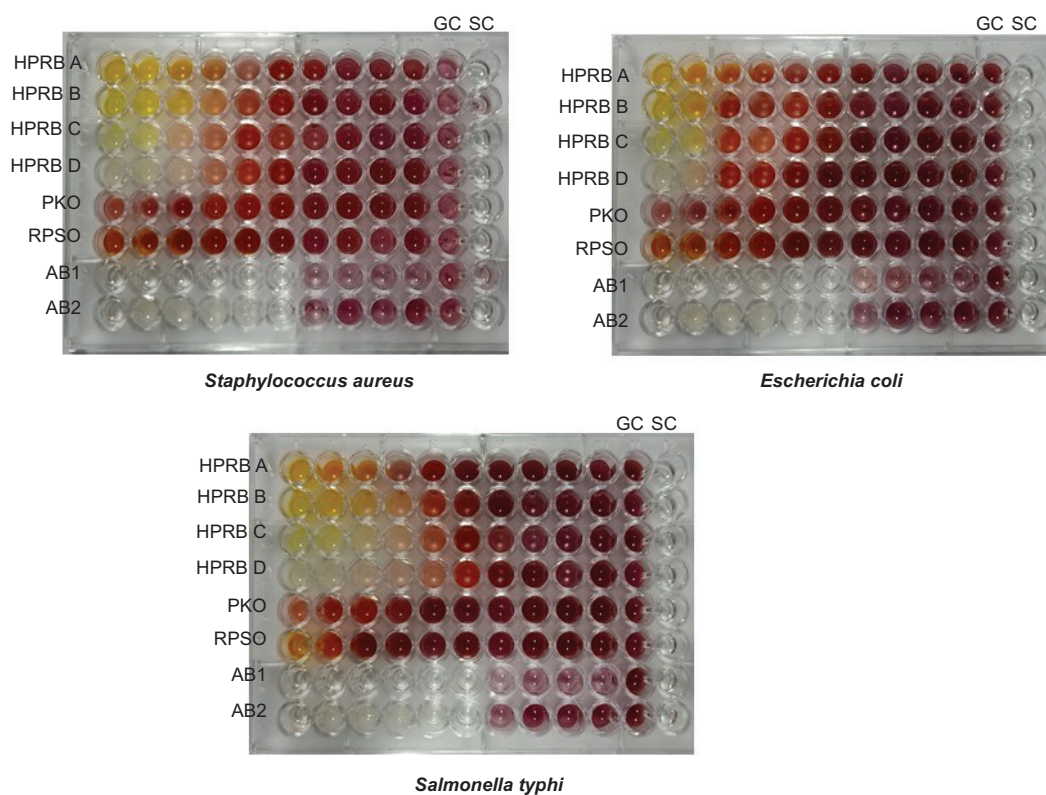


**Figure 2.** Determination of minimum inhibitory concentration (MIC) of HPRB. Bacterial growth was assessed in a 96-well plate with a gradient of decreasing HPRB concentration. The wells also contained 0.125% TTC to visualize bacterial growth. The red color indicates bacterial growth, while the absence of red color (clear or yellow wells) signifies the inhibition of bacterial growth. Antibiotic controls were included, where AB1 represents vancomycin and AB2 represents penicillin. HPRB: hydrolized palm kernel oil and red palm super olein blend; PKO: palm kernel oil; RPSO: red palm super olein.

### Bacterial staining

The microscopic images presented in Figure 3 provide a visual representation of the antibacterial efficacy of HPRB-C and HPRB-D against *S. aureus*, *E. coli*, and *S. typhi*. The untreated bacteria in positive control groups (Figures 3A, 3D, and 3G) exhibit robust growth, forming dense and confluent bacterial colonies that stain darkly with crystal violet, indicating intact cell walls. In contrast, the treated samples reveal varying degrees of bacterial inhibition that correspond to the MICs determined through quantitative assays.

For *S. aureus*, HPRB-D at 500 mg/mL (Figure 3C) visually demonstrates complete inhibition of bacterial growth, indicated by a clear background devoid of any visible bacterial colonies. Conversely, HPRB-C at the same concentration (Figure 3B) shows partial inhibition, with a few scattered and faintly stained bacterial cells still visible. These visual observations are consistent with the quantitative MIC data, which indicate a lower MIC for HPRB-D compared to HPRB-C against *S. aureus*. For *E. coli*, both HPRB-C and HPRB-D at 250 mg/mL (Figures 3E and 3F, respectively) visually confirm a significant reduction

in bacterial growth compared to the untreated control. Treatment with HPRB-D results in a clearer background with fewer and fainter bacterial cells, suggesting a more pronounced inhibitory effect compared to HPRB-C at the same concentration. This visual evidence aligns with the MIC data, where HPRB-D exhibited a lower MIC against *E. coli* than HPRB-C. In the case of *S. typhi*, both HPRB-C and HPRB-D at 500 mg/mL (Figures 3H and 3I, respectively) visually demonstrate complete inhibition of bacterial growth, resulting in a clear background with no visible bacterial colonies. This observation is consistent with the MIC data for *S. typhi*.

### Discussion

This study investigated the *in vitro* antibacterial activity of a novel blend, HPRB, against Gram-negative (*Escherichia coli* and *Salmonella typhi*) and Gram-positive (*Staphylococcus aureus*) bacteria, all of which are relevant to foodborne illnesses. Our motivation stemmed from the escalating prevalence of foodborne illnesses and the alarming rise of antibiotic-resistant

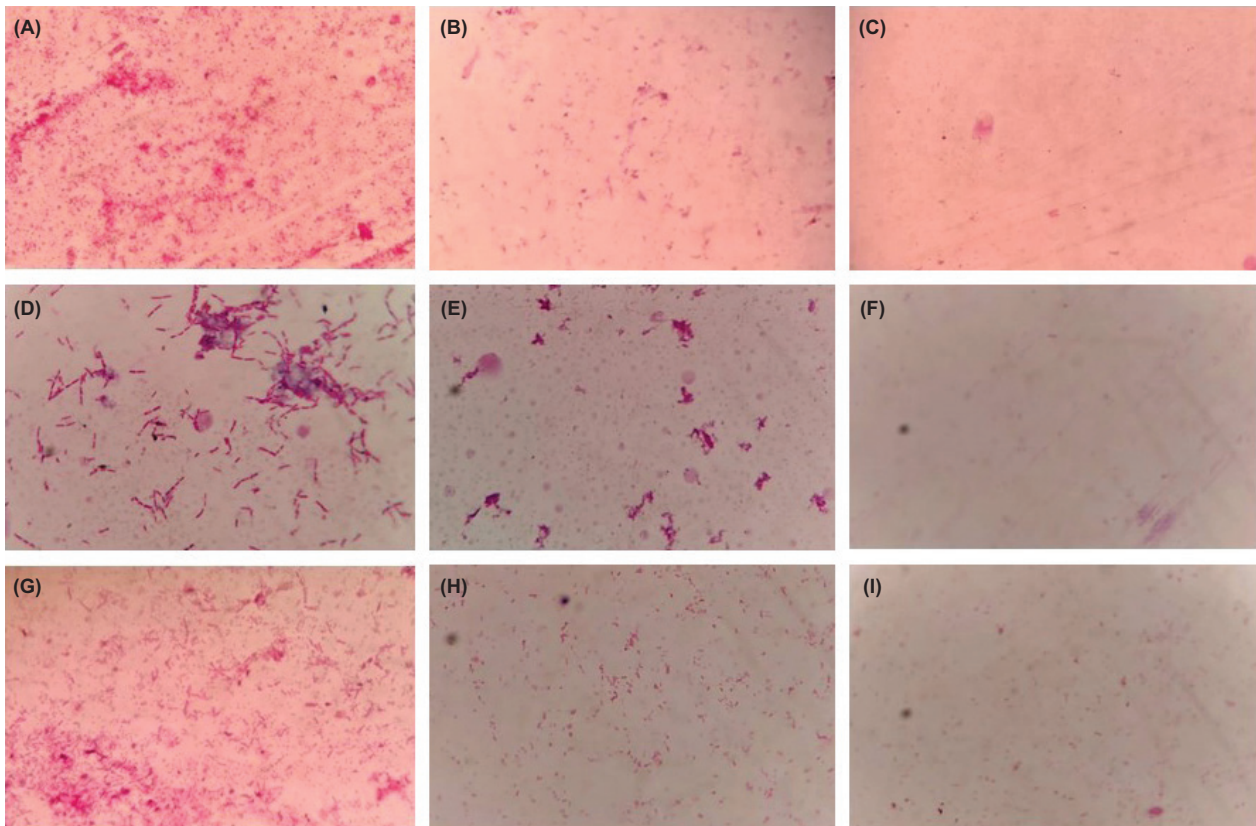


**Figure 3.** Microscopic images of bacterial cells following Gram staining: (A) untreated *S. aureus* (positive control); (B) *S. aureus* treated with HPRB-C 500, mg/mL; (C) *S. aureus* treated with HPRB-D, 500 mg/mL; (D) untreated *E. coli* (positive control); (E) *E. coli* treated with HPRB-C, 250 mg/mL; (F) *E. coli* treated with HPRB-D, 250 mg/mL; (G) untreated *S. typhi* (positive control); (H) *S. typhi* treated with HPRB-C, 500 mg/mL; and (I) *S. typhi* treated with HPRB-D, 500 mg/mL. HPRB: hydrolyzed palm kernel oil and red palm super olein blend; PKO: palm kernel oil; RPSO: red palm super olein.

bacteria, which has posed a significant threat to global health. Given the limitations of the current treatments and the urgent need for novel and sustainable antibacterial agents, this research was designed to explore the potential of natural products, specifically hydrolyzed palm oil derivatives, as promising alternatives. By comprehensively analyzing the composition of HPRB and evaluating its antibacterial activity, we aimed to identify specific components responsible for its effects and contribute to developing effective strategies against foodborne pathogens. Our hypothesis was that combining the MCFAs of PKO with the concentrated phytonutrients of RPSO through enzymatic hydrolysis would yield a potent broad-spectrum antibacterial agent with enhanced bioavailability and altered antibacterial properties. This approach builds on previous work showing the antibacterial potential of plant-derived compounds, including essential oils, polyphenols, and alkaloids, which often target multiple sites in bacterial cells, making them less prone to resistance development than single-target antibiotics.

The findings demonstrate the potent *in vitro* antibacterial activity of HPRB against *S. aureus*, *E. coli*, and *S. typhi*, providing valuable insights into its potential as a natural antibacterial agent. Notably, HPRB-C (60% PKO and 40% RPSO) and HPRB-D (80% PKO and 20% RPSO) exhibited the strongest antibacterial activity across all tested bacterial strains. This superior activity is particularly noteworthy, suggesting that the specific ratios of PKO and RPSO in these formulations are crucial for maximizing their inhibitory effects.

The observed antibacterial activity of HPRB can be primarily attributed to its unique phytochemical profile, as detailed in Tables 1–3. Specifically, the high concentrations of 1-monolaurin found in HPRB-C (17.54%) and HPRB-D (24.99%) are a key contributing factor. As a known antimicrobial compound, 1-monolaurin primarily acts against Gram-positive bacteria by integrating into and disrupting the lipid bilayer of bacterial cell membrane. This lipophilic nature facilitates its interaction with membrane lipids, altering membrane integrity,

increasing permeability, and ultimately leading to cell lysis. This mechanism is highly effective against Gram-positive bacteria because of their more susceptible thick peptidoglycan layer, compared to the outer membrane of Gram-negative bacteria. Beyond direct membrane disruption, monolaurin also inhibits bacterial growth by interfering with essential metabolic processes, such as the synthesis of vital cellular components, thus impairing replication. This dual action enhances its overall antibacterial efficacy (Wang *et al.*, 2020).

While Gram-negative bacteria, possessing an outer membrane with lipopolysaccharides (LPS), are inherently more resistant to many antimicrobial agents, including monolaurin, our study still observed activity against *E. coli* and *S. typhi*. Research suggests that monolaurin can interact with the lipid components of Gram-negative bacterial membranes, increasing permeability and potentially causing cell lysis, although often requiring higher concentrations than for Gram-positive organisms. Monolaurin may also affect Gram-negative bacterial metabolic processes by inhibiting the synthesis of essential cellular components. Furthermore, its synergistic potential with other antimicrobial agents suggests that monolaurin could enhance the effectiveness of the existing antibiotics against resistant strains (Almeida *et al.*, 2021).

Beyond 1-monolaurin, the phytonutrient content derived from RPSO, as detailed in Table 3, also significantly contributes to the observed antibacterial activity. Carotenoids, abundant in RPSO, exert antibacterial activity by modulating oxidative stress and through direct effects on bacteria, inhibiting the growth of both Gram-positive and Gram-negative species (Toti *et al.*, 2018; Viault *et al.*, 2021). The synergy between carotenoids and other bioactive compounds, such as lauric acid in MAG composition, probably amplified HPRB's overall antibacterial effects. Similarly, tocotrienols, another key component of vitamin E from RPSO, can modulate immune responses, potentially enhancing the host's ability to combat bacterial infections. They have demonstrated direct inhibitory effects against both Gram-positive and Gram-negative bacteria, including *Staphylococcus aureus*, making them promising natural antibacterial candidates. The presence of squalene, although in smaller amounts, may also contribute to the overall bioactivity (Farahmandfar *et al.*, 2019; Ismail *et al.*, 2020; Koshak *et al.*, 2024).

However, several limitations are observed while interpreting these *in vitro* results. While HPRB demonstrated promising antibacterial activity against the selected strains, it is important to acknowledge that its MIC values are considerably higher than those of the standard antibiotics (e.g., penicillin and vancomycin) used as positive controls in this study. This highlights that HPRB is

better positioned as a source of natural, broad-spectrum agents, rather than a direct replacement for conventional antibiotics in all applications. Our study also did not encompass a broader spectrum of bacteria, including other important foodborne pathogens or clinically relevant antibiotic-resistant isolates. Additionally, the interpretation of our results did not use the specific clinical breakpoints, such as those provided by CLSI, to categorize bacterial susceptibility or resistance. Instead, our findings are based on a direct comparison of inhibition zone diameters and MIC values of both positive controls, penicillin and vancomycin, showing HPRB's significant antibacterial potential (Gajic *et al.*, 2022; Hartmann *et al.*, 2020; Shrum *et al.*, 2023).

Future research should build upon the findings of this study by addressing its limitations and exploring promising avenues for further investigation. Primarily, *in vivo* studies are crucial to evaluate the therapeutic potential and safety of HPRB in complex biological systems, including animal models (Dombach *et al.*, 2022). Furthermore, investigating the potential synergy with antibiotics could offer new strategies to combat antibiotic resistance. Combining HPRB with the existing antibiotics might enhance their effectiveness and reduce the development of resistance. Considering the role of biofilms in persistent infections, future studies should examine the efficacy of HPRB in inhibiting biofilm formation and disrupting established biofilms. Biofilms are a major challenge in treating bacterial infections, and agents that can effectively target biofilms are highly valuable (Hassan Abd El-Ghany *et al.*, 2024). Additionally, efforts to achieve a more detailed identification of active compounds within HPRB, through further fractionation and purification, could help to optimize its efficacy. This could lead to the development of standardized and more potent antibacterial formulations. Finally, exploring the potential applications of HPRB in food preservation and the pharmaceutical industry warrants further investigation. The natural origin and broad-spectrum activity of HPRB make it a promising candidate for use as a food preservative to extend shelf life and reduce foodborne illnesses as well as for developing novel therapeutic agents to combat bacterial infections.

## Conclusions

This study investigated the antibacterial activity of a novel product, HPRB, against Gram-negative (*Escherichia coli* and *Salmonella typhi*) and Gram-positive (*Staphylococcus aureus*) bacteria, focusing on its composition and efficacy against common human pathogens. The production of HPRB involved the lipase-catalyzed hydrolysis of PKO and RPSO, yielding four distinct formulations (HPRB-A, HPRB-B, HPRB-C, and HPRB-D) with varied PKO and

RPSO proportions. Notably, HPRB-C (60% PKO and 40% RPSO) and HPRB-D (80% PKO and 20% RPSO) exhibited the strongest *in vitro* antibacterial activity against all three bacterial strains. This superior efficacy is primarily attributed to their high 1-monolaurin content (17.54% in HPRB-C and 24.99% in HPRB-D). Furthermore, the RPSO component significantly contributed to HPRB's antibacterial properties, potentially because of the presence of concentrated phytonutrients, including total carotene (up to 761.23 ppm in RPSO) and various vitamin E isomers (up to 1,118.17 ppm in RPSO). Microscopic images further corroborated the antibacterial efficacy of HPRB-C and HPRB-D. The findings highlight the significant potential of HPRB, particularly formulations HPRB-C and HPRB-D, as promising natural antibacterial agents, with their effectiveness stemming from the combined action of 1-monolaurin and various phytonutrients. However, further research is crucial to optimize their formulation for lower effective concentrations, investigate their *in vivo* safety and efficacy, and explore their potential applications in the food and pharmaceutical industries.

## Data Availability

Owing to privacy concerns, the datasets generated and/or analyzed in the current study are not available publicly. However, summary data and findings are present in the manuscript.

## Acknowledgments

The authors thanked the Mechanization, Post-Harvest and Environmental Conservation Research Group, particularly Oleofood Laboratory team members, for their role in this research.

## Author Contributions

Ilmi Fadhilah Rizki, Frisda Rimbun Panjaitan, Manda Edy Mulyono, and Brahmani Dewa Bajra: conceptualization; Ilmi Fadhilah Rizki, Manda Edy Mulyono, Frisda Rimbun Panjaitan, and Brahmani Dewa Bajra: methodology; Ilmi Fadhilah Rizki and Frisda Rimbun Panjaitan: validation; Ilmi Fadhilah Rizki: formal analysis; Ilmi Fadhilah Rizki: investigation; Ilmi Fadhilah Rizki: resources; Ilmi Fadhilah Rizki and Brahmani Dewa Bajra: data curation; Ilmi Fadhilah Rizki: writing—original draft preparation; Ilmi Fadhilah Rizki, Manda Edy Mulyono, Frisda Rimbun Panjaitan, and Brahmani Dewa Bajra: writing—review and editing; Ilmi Fadhilah Rizki: visualization; Ilmi Fadhilah Rizki and Frisda Rimbun Panjaitan: supervision; Ilmi Fadhilah

Rizki and Frisda Rimbun Panjaitan: project administration; Frisda Rimbun Panjaitan: fund acquisition. All authors had read and agreed to the published version of the manuscript.

## Conflicts of Interest

The authors declared no conflict of interest.

## Funding

This research was funded by Badan Pengelola Dana Perkebunan Kelapa Sawit (BPDPKS) through the Grant Riset Sawit (GRS) PRJ-363/DPKS/2022.

## References

- Abd Rashid, S.N.A., Ab. Malik, S., Embi, K., Mohd Ropi, N.A., Yaakob, H., Cheng, K.K., Sarmidi, M.R., and Leong, H.Y. 2019. Carotenoids and antioxidant activity in virgin palm oil (VPO) produced from palm mesocarp with low heat aqueous-enzyme extraction techniques. *Materials Today: Proceedings*, 42, 148–152. <https://doi.org/10.1016/j.matpr.2020.10.616>
- Almeida, A.B., Araújo, D.N., Strapazzon, J.V., Rita, C., Dilda, A., Balen, G., Deolindo, G.L., Nesi, D., Furlan, V.J.M., Pelisser, G., Mendes, R.E., Fracasso, M., Wagner, R., Boiago, M.M., and DA SILVA, A. S. 2021. Use of blend based on an emulsifier, monolaurin, and glycerides of butyric acid in the diet of broilers: Impacts on intestinal health, performance, and meat. *Anais Da Academia Brasileira de Ciencias*, 93, 1–17. <https://doi.org/10.1590/0001-3765202120210687>
- Bale, B.M., Peekate, L.P., and Wemedo, S. A. 2024. Antibiotic Susceptibility Pattern of Bacteria Associated With Clinical Waste Materials in Gokana Local Government Area of Rivers State. *Open Journal of Bioscience Research* (ISSN: 2734-2069), 5(1), 21–33. <https://doi.org/10.52417/ojbr.v5i1.577>
- Balouiri, M., Sadiki, M., and Ibsouda, S.K. (2016). Methods for *in vitro* evaluating antimicrobial activity: A review. *Journal of Pharmaceutical Analysis*, 6(2), 71–79. <https://doi.org/10.1016/j.jpha.2015.11.005>
- Cheong, N.D.H., Zakaria, L.A. and Yusof, H. 2022. Qualitative phytochemical screening and antibacterial properties of *Momordica charantia* methanolic extract against selected bacterial strains. *Malaysian Journal of Medicine and Health Sciences* 18(3), 154–161. <https://doi.org/10.47836/mjmhs18.s15.21>
- Collison, M.W. (Ed.). 2017. *Official Methods and Recommended Practices of the AOCS 7th Edition*. American Oil Chemists' Society.
- Dombach, J.L., Quintana, J.L.J., Allgood, S.C., Nagy, T.A., Gustafson, D.L., and Detweiler, C.S. 2022. A small molecule that disrupts *S. Typhimurium* membrane voltage without cell lysis reduces bacterial colonization of mice. *PLoS Pathogens*, 18(6), 1–18. <https://doi.org/10.1371/journal.ppat.1010606>

- Farahmandfar, R., Esmailzadeh Kenari, R., Asnaashari, M., Shahrampour, D., and Bakhshandeh, T. 2019. Bioactive compounds, antioxidant and antimicrobial activities of *Arum maculatum* leaves extracts as affected by various solvents and extraction methods. *Food Science and Nutrition*, 7(2), 465–475. <https://doi.org/10.1002/fsn3.815>
- Gajic, I., Kabic, J., Kekic, D., Jovicevic, M., Milenkovic, M., Mitic Culafic, D., Trudic, A., Ranin, L., and Opavski, N. 2022. Antimicrobial Susceptibility Testing: A Comprehensive Review of Currently Used Methods. *Antibiotics*, 11(4), 1–26. <https://doi.org/10.3390/antibiotics11040427>
- Ghany, S.S.H.A.E., Ibrahim, R.A., El-Gendy, A.O., El-Baky, R.M.A., Mustafa, A., and Azmy, A.F. 2024. Novel synergistic interactions between monolaurin, a mono-acyl glycerol and  $\beta$  lactam antibiotics against *Staphylococcus aureus*: an in vitro study. *BMC infectious diseases*, 24(1), 379. <https://doi.org/10.1186/s12879-024-09261-9>
- Grajzer, M., Kozłowska, W., Zalewski, I., Matkowski, A., and Monika, R. 2025. Nutraceutical Prospects of Pumpkin Seeds: A Study on the Lipid Fraction Composition and Oxidative Stability Across Eleven Varieties. 1–21.
- Habibiasr, M., Mokhtar, M.N., Ibrahim, M.N., Yunos, K.F.M. and Ibrahim, N.A. 2022. Effect of drying on the physical and chemical properties of palm kernel oil. *Journal of Science of Food and Agriculture* 102(10), 4046–4053. <https://doi.org/10.1002/jsfa.11753>
- Hartmann, M.S., Mousavi, S., Bereswill, S. and Heimesaat, M.M. 2020. Vitamin E as promising adjunct treatment option in the combat of infectious diseases caused by bacterial including multi-drug resistant pathogens—results from a comprehensive literature survey. *European Journal of Microbiology and Immunology* 10(4), 193–201. <https://doi.org/10.1556/1886.2020.00020>
- Hassan Abd El-Ghany, S.S., Azmy, A.F., Osama El-Gendy, A., Abd El-Baky, R.M., Mustafa, A., Abourehab, M.A.S., El-Beeh, M.E., and Ibrahim, R.A. 2024. Antimicrobial and Antibiofilm Activity of Monolaurin against Methicillin-Resistant *Staphylococcus aureus* Isolated from Wound Infections. *International Journal of Microbiology*, 2024. <https://doi.org/10.1155/2024/7518368>
- Hovorková, P., Laloučková, K., & and Skřivanová, E. (2018). Determination of *in vitro* antibacterial activity of plant oils containing medium-chain fatty acids against Gram-positive pathogenic and gut commensal bacteria. *Czech Journal of Animal Science*, 63(3):119–125. <https://doi.org/10.17221/70/2017-CJAS>
- Ismail, M., Alsalahi, A., Imam, M.U., Ooi, D.J., Khaza'ai, H., Aljaberi, M.A., Shamsudin, M.N., and Idrus, Z. 2020. Safety and Neuroprotective Efficacy of Palm Oil and Tocotrienol-Rich Fraction from Palm Oil: A Systematic Review. *Nutrients*, 12(521). <https://doi.org/10.3390/nu12020521>
- Jackman, J.A., Yoon, B.K., Li, D. and Cho, N.J. 2016. Nanotechnology formulations for antibacterial free fatty acids and monoglycerides. *Molecules* 21(3). <https://doi.org/10.3390/molecules21030305>
- Karpiński, T.M. and Adamczak, A. 2019. Fucoxanthin—an antibacterial carotenoid. *Antioxidants* 8(8), 239. <https://doi.org/10.3390/antiox8080239>
- Koshak, A.E., Elfaky, M.A., Abdallah, H.M., Albadawi, D.A.I., Mohamed, G.A., Ibrahim, S.R.M., Alzain, A.A., Khafagy, E.S., Rajab, A.A.H., and Hegazy, W.A.H. 2024. Arctigenin from Burdock Root Exhibits Potent Antibacterial and Anti-Virulence Properties against *Pseudomonas aeruginosa*. *Journal of Microbiology and Biotechnology*, 34(8), 1642–1652. <https://doi.org/10.4014/jmb.2403.03003>
- Lee, H., and Yoon, Y. 2021. Etiological agents implicated in food-borne illness world wide. *Food Science of Animal Resources*, 41(1), 1–7. <https://doi.org/10.5851/KOSFA.2020.E75>
- Li, X., Gao, Y., Wang, S., Huang, Y., Long, G., Wang, D., Jia, J. and Wang, A. 2024. Natural prenylflavonoids from *Sophora flavescens* root bark against multidrug. *Journal of Agricultural and Food Chemistry*, 72(26), 14684–14700.
- Martins, G.A., and Bicas, J.L. 2024. Antifungal activity of essential oils of tea tree, oregano, thyme, and cinnamon, and their components. *Brazilian Journal of Food Technology*, 27, 1–15. <https://doi.org/10.1590/1981-6723.07123>
- Monteiro, J.B., Nascimento, M.G., and Ninow, J.L. 2003. Lipase-catalyzed synthesis of monoacylglycerol in a homogeneous system. *Biotechnology Letters*, 25(8), 641–644. <https://doi.org/10.1023/A:1023016215537>
- Mulyadarsono, N.D.A.R., and Kristopo, H. 2024. The Water Hygiene of Street Food Vendors in Southeast Asia: A Review. *IOP Conference Series: Earth and Environmental Science*, 1324(1), 1–8. <https://doi.org/10.1088/1755-1315/1324/1/012104>
- Mulyono, M.E., Lubis, M.E.S., Yudianto, B.G., Panjaitan, F.R., Rizki, I.F. and Bajra, B.D. 2023. Application of dry fractional crystallisation on high-oleic low-palmitic red palm super olein production. *International Journal of Food Science and Technology* 58(6), 3402–3409. <https://doi.org/10.1111/ijfs.16353>
- Ngatirah, N., Hidayat, C., Rahayu, E.S. and Utami, T. 2022. Enzymatic glycerolysis of palm kernel olein-stearin blend for monolaurin synthesis as an emulsifier and antibacterial. *Foods* 11(16). <https://doi.org/10.3390/foods11162412>
- Okafor Chibuanuli, M., Ikegbunam Moses, N., Nwachukwu Judith, C., Ebenebe Ijeoma, N. and Nnanna Joy, C. 2020. Prevalence of antibiotic resistant bacteria in Nigerian fermented food condiments. *Journal of Biology and Life Science* 11(1), 110. <https://doi.org/10.5296/jbls.v11i1.16383>
- Performance Standards for Antimicrobial Susceptibility Testing 30th Edition. 2020. In *Clinical and Laboratory Standards Institute*.
- Pranav, R.J., Kumar, S.S., Rangaraj, P.R., Sangapillai, K., and Ragunathan, R. 2024. Exploring the therapeutic potential of cinnamon and clove essential oils for mitigating food-borne diseases: bioactivity and molecular interactions. *Food Science and Applied Biotechnology*, 7(1), 122–132. <https://doi.org/10.30721/fsab2024.v7.i1.318>
- Shrum, S.A., Nukala, U., Shrimali, S., Pineda, E.N., Krager, K.J., Thakkar, S., Jones, D.E., Pathak, R., Breen, P.J., Aykin-Burns, N. and Compadre, C.M. 2023. Tocotrienols provide radioprotection to multiple organ systems through complementary mechanisms of antioxidant and signaling effects. *Antioxidants* 12(11), 1987. <https://doi.org/10.3390/antiox12111987>

- Smith, A., & Hussey, M. 2016. Gram Stain Protocols. In *American Society for Microbiology* (Issue September 2020).
- Subroto, E. 2020. Monoacylglycerols and diacylglycerols for fat-based food products: a review. *Food Research* 4(4), 932–943. [https://doi.org/10.26656/fr.2017.4\(4\).398](https://doi.org/10.26656/fr.2017.4(4).398)
- Takó, M., Kerekes, E.B., Zambrano, C., Kotogán, A., Papp, T., Krisch, J., and Vágvolgyi, C. 2020. Plant phenolics and phenolic-enriched extracts as antimicrobial agents against food-contaminating microorganisms. *Antioxidants*, 9(2). <https://doi.org/10.3390/antiox9020165>
- Tanasă, F., Nechifor, M., & Teacă, C.A. 2024. Essential Oils as Alternative Green Broad-Spectrum Biocides. *Plants*, 13(23). <https://doi.org/10.3390/plants13233442>
- Tao, Q., Wu, Q., Zhang, Z., Liu, J., Tian, C., Huang, Z., Malakar, P.K., Pan, Y., and Zhao, Y. (2022). Meta-Analysis for the Global Prevalence of Foodborne Pathogens Exhibiting Antibiotic Resistance and Biofilm Formation. *Frontiers in microbiology*, 13, 906490. <https://doi.org/10.3389/fmicb.2022.906490>
- Thamlikitkul, V., Tiengrim, S., Thamthaweechok, N., Buranapakdee, P., and Chiemchaisri, W. 2019. Contamination by antibiotic-resistant bacteria in selected environments in Thailand. *International Journal of Environmental Research and Public Health*, 16(19). <https://doi.org/10.3390/ijerph16193753>
- Tian, F., Woo, S.Y., Lee, S.Y., Park, S.B., Zheng, Y., and Chun, H.S. 2022. Antifungal Activity of Essential Oil and Plant-Derived Natural Compounds against *Aspergillus flavus*. *Antibiotics*, 11(12). <https://doi.org/10.3390/antibiotics11121727>
- Toti, E., Oliver Chen, C.Y., Palmery, M., Valencia, D.V., and Peluso, I. 2018. Non-provitamin A and provitamin A carotenoids as immunomodulators: Recommended dietary allowance, therapeutic index, or personalized nutrition? *Oxidative Medicine and Cellular Longevity*, 2018. <https://doi.org/10.1155/2018/4637861>
- Tsukagoshi, M., Sirisopapong, M., Namai, F., Ishida, M., Okrathok, S., Shigemori, S., Ogita, T., Sato, T., Khempaka, S., and Shimosato, T. 2020. *Lactobacillus ingluviei* C37 from chicken inhibits inflammation in LPS-stimulated mouse macrophages. *Animal Science Journal*, 91(1), 1–7. <https://doi.org/10.1111/asj.13436>
- Ustadi, F.F., Widodo, A.D.W. and Setiawati, Y. 2022. *In vitro* antibacterial activity of waste palm cooking oil against *Staphylococcus aureus*. *Indian Journal of Forensic Medicine & Toxicology* 16(1), 487–493.
- Viault, G., Kempf, M., Ville, A., Alsabil, K., Perrot, R., Richomme, P., Hélesbeux, J.J., and Séraphin, D. 2021. Semisynthetic Vitamin E Derivatives as Potent Antibacterial Agents against Resistant Gram-Positive Pathogens. *ChemMedChem*, 16(5), 881–890. <https://doi.org/10.1002/cmdc.202000792>
- Wang, W., Chen, J., Shao, X., Huang, P., Zha, J., and Ye, Y. 2021. Occurrence and antimicrobial resistance of *Salmonella* isolated from retail meats in Anhui, China. *Food Science and Nutrition*, 9(9), 4701–4710. <https://doi.org/10.1002/fsn3.2266>
- Wang, W., Wang, R., Zhang, G., Chen, F., and Xu, B. 2020. *In vitro* antibacterial activities and mechanisms of action of fatty acid monoglycerides against four foodborne bacteria. *Journal of Food Protection*, 83(2), 331–337. <https://doi.org/10.4315/0362-028X.JFP-19-259>
- World Health Organization (WHO). 2016. Burden of Foodborne Diseases in the South-East Asia Region. WHO library cataloguing-in-publication data. WHO, Geneva, Switzerland.
- Wu, Y. and Zeng, Z. 2024. Antibiotic residues, antimicrobial resistance and intervention strategies of foodborne pathogens. *Antibiotics* 13(4), 1–7. <https://doi.org/10.3390/antibiotics13040321>
- Wu, L., Zhao, J., Wu, L., Zhang, Y., and Li, J. 2022. Simultaneous determination of squalene, tocopherols and phytosterols in edible vegetable oil by SPE combined with saponification and GC-MS. *Lwt*, 169(September), 114026. <https://doi.org/10.1016/j.lwt.2022.114026>
- Wu, Y., and Zeng, Z. 2024. Antibiotic Residues, Antimicrobial Resistance and Intervention Strategies of Foodborne Pathogens. *Antibiotics*, 13(4), 1–7. <https://doi.org/10.3390/antibiotics13040321>
- Zeng, F.K., Yang, B., Wang, Y.H., Wang, W.F., Ning, Z.X., and Li, L. 2010. Enzymatic production of monoacylglycerols with camellia oil by the glycerolysis reaction. *Journal of the American Oil Chemists' Society*, 87(5), 531–537. <https://doi.org/10.1007/s11746-009-1533-x>